Quantum Electronics **50** (7) 683–687 (2020)

LASERS

https://doi.org/10.1070/QEL17245

Optically pumped semiconductor laser based on a type-II CdS/ZnSe heterostructure

M.R. Butaev, V.I. Kozlovsky, Ya.K. Skasyrsky

Abstract. **An optically pumped semiconductor laser based on a type-II CdS/ZnSe nanoheterostructure containing 10 quantum wells (QWs) was studied. The structure was grown by metal-organic vapour phase epitaxy on a GaAs substrate. The lifetime of electron-hole pairs at a low pump level was measured by luminescence decay to be ~10 ns. The peak power of the microcavity semiconductor laser at room temperature and longitudinal pumping by a repetitively pulsed N_2 laser was 7.2 W at a wavelength of 514 nm. The relatively low laser slope efficiency (0.35%) is explained by amplified spontaneous emission propagating along the structure. The peak power and efficiency of the laser in the case of transverse pumping increase to 70 W and 3.5%, respectively.**

Keywords: *MOVPE, semiconductor laser, CdS/ZnSe heterostructure, quantum wells, optical pumping.*

1. Introduction

The development of semiconductor disk lasers (SDLs), or vertical-external-cavity surface-emitting semiconductor lasers, in particular, with optical pumping, is related to their ability to generate high-power radiation in a wide spectral range with a high (diffraction-limited) beam quality [1–4]. Despite the fact that the present-day SDL structures are based mainly on III–V compounds emitting in the near-IR region, the possibility of using various nonlinear effects in their cavities allows them to operate in the UV [5, 6], visible [3, 4], mid-IR [7], and terahertz [8] spectral regions.

The aim of the present work is to develop optically pumped SDLs based on II–VI heterostructures with the fundamental wavelength in the blue–green spectral range (480–560 nm). In this case, wavelength conversion to the mid-UV spectral range (240–280 nm), which is most popular for some applications, can be achieved by relatively simple intracavity frequency doubling. For this purpose, it is necessary to use resonant periodic structures of wide-gap compounds as the active laser medium. The use of the third or fourth harmonic of SDLs based on III–V structures considerably decreases the efficiency of the laser system as a whole [5, 9].

M.R. Butaev, V.I. Kozlovsky Lebedev Physical Institute, Russian Academy of Sciences, Leninsky prosp. 53, 119991 Moscow, Russia; National Research Nuclear University MEPhI, Kashirskoe sh. 31, 115409 Moscow, Russia; e-mail: vikoz@sci.lebedev.ru;
Ya.K. Skasyrsky Lebedev Physical Institute, Russian Academy of Sciences, Leninsky prosp. 53, 119991 Moscow, Russia

Received 16 January 2020
Kvantovaya Elektronika **50** (7) 683–687 (2020)
Translated by M.N. Basieva

Ones of the well-known wide-gap materials corresponding to the mentioned range are ZnSe-based compounds [10], which were considered at the end of the last century as the most promising media for blue–green laser diodes (LDs) [11, 12]. However, the problem of degradation of LDs based on II–VI compounds is still unsolved. To degradation factors, apart from those typical for injection lasers, in which it is necessary to form the p–n junction and reliable contacts, one assigns insufficiently strong chemical bonds between the second-group metal atoms and selenium and internal elastic stresses in quantum wells (QWs) [10, 13, 14]. Only the last factors can play an important role in degradation of optically pumped lasers.

An alternative to the structures based on II–VI compounds for the blue–green spectral range are the InGaN/GaN structures. At present, blue LDs with a power of several watts are commercially available. However, to fabricate SDLs, it is necessary either to use a structure with an integrated Bragg mirror or to be able to separate the grown structure from the substrate (usually from sapphire) and transfer it to another substrate with a high thermal conductivity, like diamond or silicon carbide. In both cases, it is necessary to solve severe technological problems. In contrast to the structures of nitride compounds, the II–VI structures can be easily separated from the GaAs growth substrate owing to the existence of selective etching solutions for GaAs.

In [15, 16] we studied the possibility of using the ZnCdS/ZnSSe type-II heterojunction in semiconductor lasers, in particular, in microcavity laser with electron-beam pumping. It was suggested that these heterostructures, in contrast to the previously studied Zn(Cd)Se/Zn(Mg)Se heterostructures [10, 17], are less susceptible to solid-phase diffusion at epitaxial growth temperatures and at intense excitation owing to the presence of more stable sulphur chemical bonds. At a particular composition of QWs and barriers, namely, $Zn_{0.4}Cd_{0.6}S/ZnS_{0.06}Se_{0.94}$, all layers of this heterostructure can be almost completely matched to the GaAs substrate in crystal lattice parameters, which considerably reduces internal stresses. Investigations showed that the lasers based on ZnCdS/ZnSSe heterostructures successfully operate in the blue spectral region but their wavelength is limited by a value of about 490 nm. The longer-wavelength green region can be reached by decreasing the Zn concentration in the ZnCdS QW. In this connection, we are studying the CdS/ZnSe heterostructure as a potentially active medium for green semiconductor lasers.

Another important advantage of the CdS/ZnSe heterostructure is a small jump in the refractive index at the heterointerfaces. This makes it possible to weaken an effect of the cavity mode displacement from the gain peak because of forming the band gap of the photonic crystal (which is a peri-

odic structure) and thus to achieve the minimum lasing threshold attainable in the case of resonant-periodic gain [18]. A potentially useful property is also a low internal absorption in the case of nonuniform pumping of QWs, which is related to the specific features of the energy band diagram of the considered heterostructure. However, it should be noted that this heterostructure belongs to the type-II heterostructures, which leads to spatial separation of charge carriers generated by pumping, because of which the radiative recombination rate decreases and the lasing threshold may increase.

In the present paper, we report the results of investigation of a semiconductor laser based on a CdS/ZnSe nanoheterostructure upon both longitudinal pumping of a microcavity and transverse pumping of a cleaved-facet cavity by a nitrogen laser (337 nm). These results demonstrate the possibility of using this structure as an active medium of green semiconductor lasers, which is a basis for subsequent development of SDLs with this structure.

2. Experiment

The CdS/ZnSe nanoheterostructures were grown by metal-organic vapour-phase deposition in a hydrogen flow at atmospheric pressure in a quartz reactor. The design of the studied heterostructures is schematically shown in Fig. 1a. As initial compounds for the growth of the structures we used dimethyl selenide $(CH_3)_2Se$, dimethyl cadmium $(CH_3)_2Cd$, diethyl sulfide $(C_2H_5)_2S$, and diethyl zinc $(C_2H_5)_2Zn$. The structures were grown on GaAs substrates disoriented from the (001) to the (111)A plane by 10°; the substrate temperature was 440 °C. The thicknesses of layers were controlled during growth by measuring reflection of the 650-nm LD radiation focused into a spot 2 mm in diameter on the growth substrate. The thicknesses of the ZnSe and CdS layers at control points were 5 and 4 nm, respectively. The thicknesses of the ZnS_xSe_{1-x} barrier layers between the three-layer QWs were grown to be 86 nm, so that the structure period would be about 100 nm, which corresponded to achieving resonant-periodic gain, i.e., to half of the wavelength inside the laser structure. The first ZnS_xSe_{1-x} layer on the growth substrate was approximately 193 nm thick, while the thickness of the last layer was close to 93 nm. However, the thicknesses of the layers could smoothly vary over the structure surface due to the inhomogeneous flow of hydrogen with initial components in the reactor. Elastic stresses caused by QWs were compensated by increasing the sulphur concentration in the barriers to 11%. The total thickness of the heterostructure with 10 QWs was approximately 1.2 μm. The heterostructures had mirror-smooth surfaces.

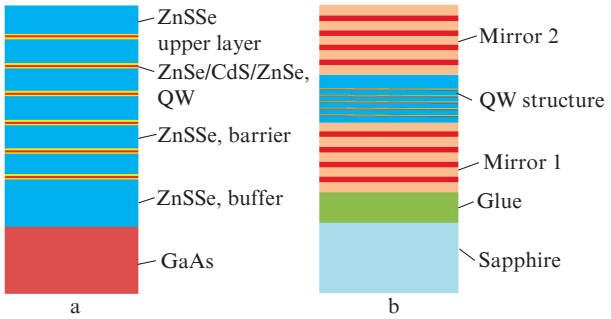

Figure 1. Schematic of (a) the structure and (b) active element with the microcavity.

The active element of the microcavity laser (Fig. 1b) was fabricated as follows. The first dielectric mirror consisting of 11 HfO_2–SiO_2 layer pairs with calculated reflection coefficient $R = 99.5\%$ for wavelength $\lambda = 515$ nm was deposited on the structure heated to 200 °C. The structure was glued with this mirror to the sapphire substrate 5 mm thick using EPOTEK-301 optical epoxy. Then, the GaAs growth substrate was removed and the second dielectric mirror consisting of 12 layer pairs with $R = 99.5\%$ at $\lambda = 515$ nm was deposited on the free surface of the structure without heating. The thicknesses of the mirrors were approximately 1.7 and 1.8 μm, respectively. The transmission spectra of the mirrors measured using control glass (mirror 1) and sapphire (mirror 2) substrates are presented in Fig. 2. The reflection minima turned out to be shifted from the given wavelength (515 nm). In addition, heating of the structure considerably increases the refractive index of HfO_2, because of which the minimum transmission coefficient of mirror 1 was noticeably lower than that of mirror 2, although the latter had more layer pairs. From experimental curves, we calculated the transmission coefficients of mirrors for a plane wave incident from the structure. These coefficients for a wavelength of 515 nm were found to be approximately 0.6%. The transmission of the mirrors at the pump laser wavelength (337 nm) exceeded 80%.

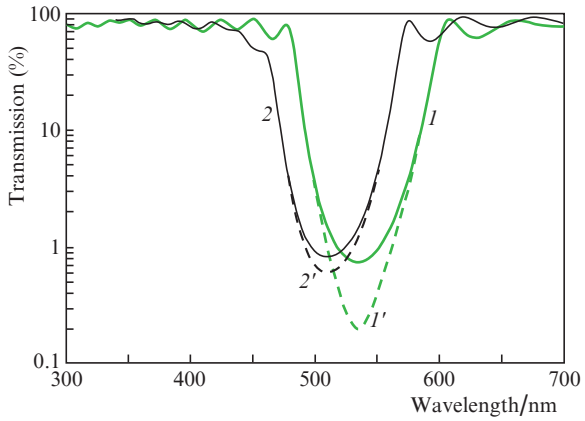

Figure 2. Transmission spectra of the (*1*) first and (*2*) second mirrors measured with control sapphire and glass substrates, as well as (*1′* and *2′*) corresponding calculated transmission spectra for a plane wave incident on mirrors 1 and 2 from the structure.

It should be noted that the thicknesses of the mirrors and the glue layer considerably exceed the structure thickness. This may lead to additional elastic stresses in the structure. As a result, rare cracks appeared along the [110] and [1-10] directions as is seen in Fig. 8a for a structure with an area of 1–2 cm^2.

The microcavity structure was longitudinally excited through the sapphire substrate by an LGI-21 nitrogen laser or by a higher-power LGI-503 laser ($\lambda = 337$ nm). Figure 3 presents the optical scheme of the laser and the system for measuring the peak power of the pump and laser pulses. We used two coaxial photoelectric detectors (CPDs) to separately record the oscillograms of pump and lasing pulses. The peak pump power was first measured in relative units and then the

obtained data were correlated to the measured peak pump power passed through the lens, sapphire substrate, mirror 1, and glue layer minus the power passed through the entire active element. The latter value did not exceed 5% of the incident power. The delay between the pump and lasing pulses was corrected taking into account the different lengths of the used coaxial cables and different distances from the CPDs to the radiation source. The laser radiation was filtered by TF-5 glass 10 mm thick, which completely cut off the pump radiation. The radiation spectrum was recorded by an MDR-4 monochromator equipped with a linear CCD array.

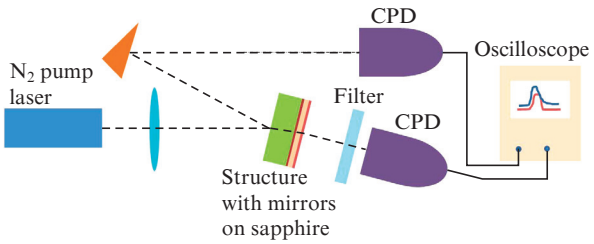

Figure 3. Optical scheme of the laser.

3. Experimental results and discussion

Figure 4 shows the emission spectra of the M-76 structure with a microcavity and without mirrors at different pump levels.

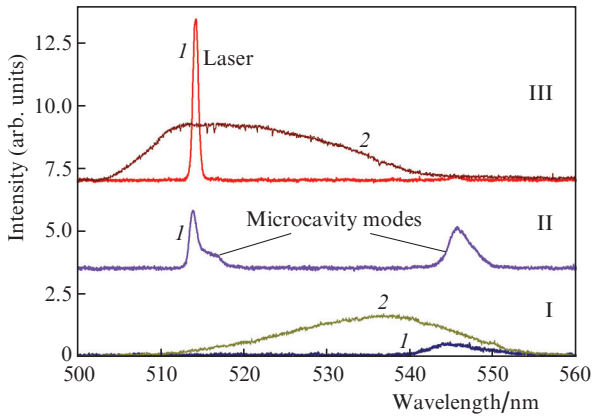

Figure 4. Emission spectra of the M-76 structure (*1*) with a microcavity and (*2*) without mirrors at different pump levels: (I) subthreshold, (II) threshold, and (III) above threshold.

With increasing pump level, the spontaneous emission spectrum shifts to short wavelengths, which is typical for type-II heterostructures [15, 19]. The microcavity is actually a filter for spontaneous emission and transmits its only in eigenmodes. Because of this, the microcavity spectrum at low pump levels contains only one mode peaking near 545 nm. At a higher pump level, spontaneous emission can yield two modes, near 545 and 515 nm. The lasing threshold is achieved for the mode peaking at 515 nm. Above the threshold, lasing is observed in a narrow line with a maximum at 514 nm and a full width at half maximum (FWHM) smaller than 1 nm. Lasing in other structures was observed at wavelengths of 519 and 537 nm.

Figure 5 shows the oscillograms of pump and microcavity laser pulses at a peak pump power $I_p \approx 1$ MW cm^{-2}, as well as of the structure without mirrors at $I_p \approx 2$ kW cm^{-2}. The FWHM of the pump pulse was ~ 8 ns, and the laser pulse FWHM was approximately 4 ns. The laser pulse maximum almost coincided with to the pump pulse maximum. The spontaneous emission pulse was shifted from the pump pulse and demonstrated a close-to-exponential decay with a characteristic time of 9.5 ns.

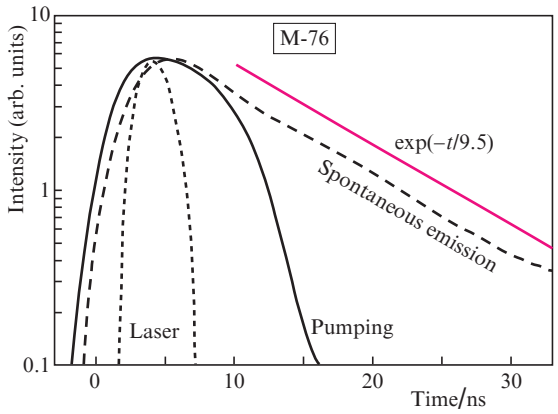

Figure 5. Oscillograms of a pump pulse, a microcavity laser pulse upon peak pump intensity $I_p \approx 1$ MW cm^{-2}, and a pulse of the structure without mirrors at $I_p \approx 2$ kW cm^{-2} on a logarithmic scale. The straight line corresponds to the exponential luminescence decay with a characteristic time of 9.5 ns.

The dependence of the laser pulse peak power emitted from the free microcavity surface on the incident pump power is presented in Fig. 6. The excited region diameter was ~0.5 mm. At a diameter smaller than 0.5 mm and the maximum pump power, we observed catastrophic degradation of the structure. The maximum laser peak power was 3.9 W. In this case, the power emitted from the sapphire substrate was 3.3 W. The total laser peak power was 7.2 W at a pump pulse peak power of 2195 W. The lasing threshold determined from the linear approximation of the dependence of the laser power

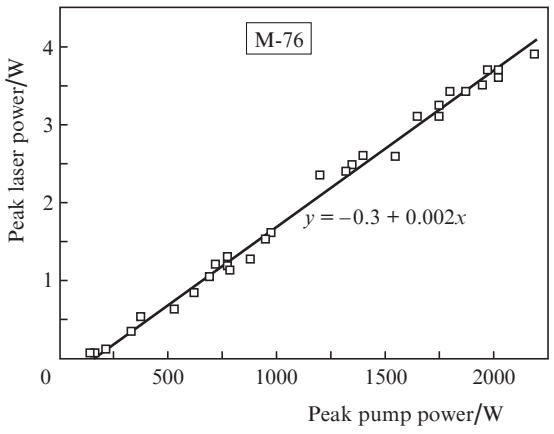

Figure 6. Dependence of the peak laser pulse power on the incident peak pump power.

on the pump power was 154 W. From this, the laser slope efficiency was estimated to be 0.35%. As the excitation spot size decreased to 300 μm and lower pump powers, the efficiency increases to 0.6%. We think that the main reason for the rather low laser efficiency is the amplified spontaneous emission propagating along the structure.

Figure 7a shows a photograph of the near-field laser spot at a small excess over the lasing threshold. One can see that lasing occurs in separate points with cross sections below 10 μm. These points are spatially incoherent with each other and correspond to independent lasers. The lasing threshold corresponding to the appearance of bright points in the near-field zone is ~100 kW cm^{-2}.

The far-field intensity distribution of such lasers is axially symmetric with a characteristic angular divergence of 10°. This distribution photographed with a digital camera without objective at a distance of 10 cm from the structure is shown in Fig. 7c. However, in addition to the laser radiation, we observe intense amplified spontaneous emission propagating at a large angle to the normal to the microcavity. This emission was recorded on a paper sheet at a distance of 2 mm from the microcavity surface (Fig. 7b). The central spot size corresponds to the laser beam divergence, and the halo around this spot is caused by spontaneous emission. The spontaneous emission power is comparable to the laser power.

An additional evidence of the influence of amplified spontaneous emission on the laser efficiency is that the pump-to-laser power conversion efficiency increases in the case of transverse pumping of the structure. In these experiments, the upper microcavity mirror was etched away with hydrofluoric acid. The cavity was formed by the cleavages appeared as a result of aforementioned cracking of the structure. A photograph of the near-field radiation of the cracked structure excited by a pump beam ~1.5 mm in diameter is presented in Fig. 8a. One can see that intense radiation is emitted from cleavages in the region of excitation.

Figure 8b presents a photograph of an emitting active element excited by a nitrogen laser. The active element is mounted on a sapphire disc 20 mm in diameter, whose surfaces are perpendicular to the photograph plane. The structure is mounted on the right side of the disk, and pumping occurs from the left through the sapphire disc. Behind the disc, a white paper sheet is placed parallel to the normal to the sapphire disk. On this sheet, one can observe the laser radiation under transverse pumping. The maximum measured power in one direction exceeded 35 W. Assuming that the power in the opposite direction is approximately the same, we obtain the laser efficiency to be about 3.5%, which is an order of magnitude higher than in the case of longitudinal pumping.

Figure 9 shows the spectra of transversely optically pumped lasers based on two different structures.

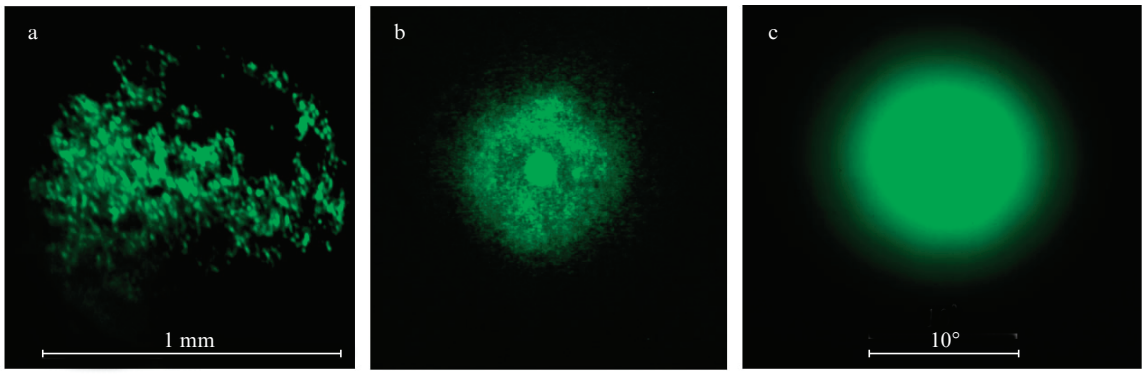

Figure 7. Photographs of the (a) near-field laser spot, (b) microcavity radiation pattern on a paper sheet placed at a distance of 2 mm from the microcavity surface, and (c) far-field laser radiation intensity distribution.

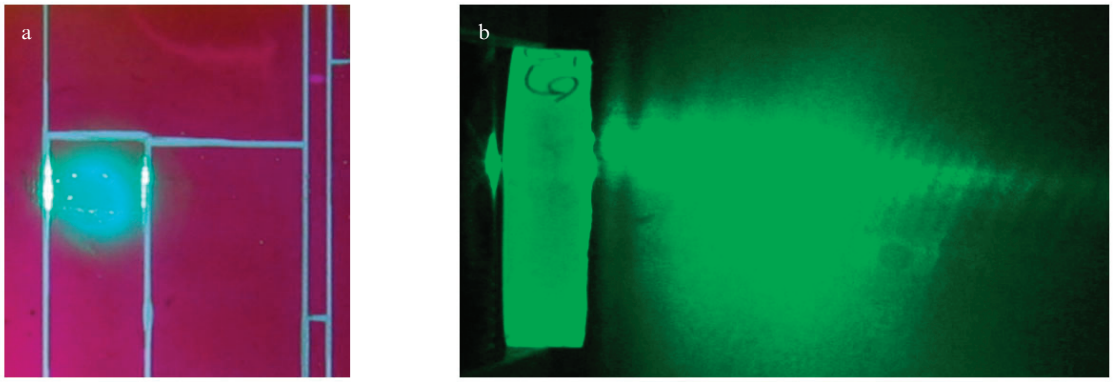

Figure 8. Photographs of (a) the near-field radiation of the transversely optically pumped laser and (b) emitting active element (the structure is mounted on the right surface of the sapphire disc; the pump beam is incident from the left through sapphire; the transversely pumped laser radiation is observed on a paper sheet placed behind the sapphire disc parallel to the normal to the disc).

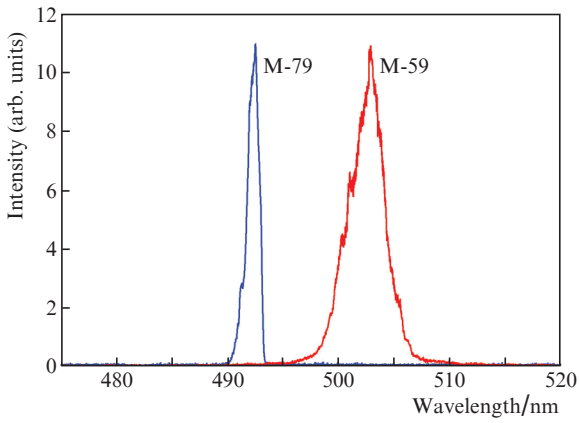

Figure 9. Spectral of transversely optically pumped lasers based on the M-59 and M-79 structures.

4. Conclusions

We fabricated for the first time a green semiconductor laser based on the type-II CdS/ZnSe/ZnSSe nanoheterostructure operating with both longitudinal and transverse pumping of the microcavity by a nitrogen laser. The investigation results show that, despite the type II band offset, the studied heterostructure is promising for developing optically pumped green semiconductor lasers. The output power in the case of longitudinal pumping of the microcavity exceeded 7 W. The low laser efficiency (0.35%) in this geometry is related to the parasitic amplification of spontaneous emission along the structure. The laser power and efficiency increase by an order of magnitude in the case of transverse pumping of the structure. Further increase in these parameters can be achieved by improving the heterostructure quality and optimising the pumping conditions and the cavity parameters.

Acknowledgements. This work was supported by the Competitiveness Enhancement Programme of the National Research Nuclear University MEPhI (Grant No. 02. a03.21.0005). We are grateful to P.I. Kuznetsov for consultations on epitaxial growth of II–VI heterostructures.

References

1. Kuznetsov M., Hakimi F., Sprague R., Mooradian A. *IEEE Photon. Techn. Lett*., **9**, 1063 (1997).
2. Tropper A.C., Hoogland S. *Progr. Quantum Electron*., **30**, 1 (2006).
3. Okhotnikov O.G. *Semiconductor Disk Lasers: Physics and Technology* (Weinheim: Wiley-VCH, 2010).
4. Hastie J.E., Calvez S., Dawson M.D., in *Semiconductor Lasers* (Woodhead Publ. Limited, 2013) Vol. 9, p. 341.
5. Shu Qi-Ze, Caprara Andrea L., Berger Jill D., Anthon Douglas W., Jerman Hal, Spinelli Luis. *Proc. SPIE*, **7193**, 719319 (2009).
6. Rodríguez-García Julio M., Paboeuf David, Hastie Jennifer E. *IEEE J. Sel. Top. Quantum Electron*., **23** (6), 5100608 (2017).
7. Stothard D.J.M., Hopkins J-M., Burns D., Dunn M.H. *Opt. Express*, **17** (13), 10648 (2009).
8. Scheller Maik, Yarborough Joe M., Moloney Jerome V., Fallahi Mahmoud, Koch Martin, Koch Stephan W. *Opt. Express*, **18** (26), 27112 (2010).
9. Kaneda Yushi, Wanga Tsuei-Lian, Yarborougha J.M., Fallahia Mahmound, Moloneya Jerome V., Yoshimurab Masashi, Morib Yusuke, Sasaki Takatomo. *Proc. SPIE*, **7193**, 719318 (2009).
10. Ivanov S.V., Sorokin S.V., Sedova I.V., in *Molecular Beam Epitaxy* (Elsevier Inc., 2018) Vol. 25, p. 571.
11. Haase M.A., Qiu J., DePuydt J.M., Cheng H. *Appl. Phys. Lett*., **59** (11), 1272 (1991).
12. Kato E., Noguchi H., Nagai M., Okuyama H., Kijima S., Ishibashi A. *Electron. Lett*., **34** (3), 282 (1998).
13. Waag A., Litz Th., Fischer F., Lugauer H.-J., Baron T., Schüll K., Zehnder U., Gerhard T., Lunz U., Keim M., Reuscher G., Landwehr G. *J. Cryst. Growth*, **184–185**, 1 (1998).
14. Law K.-K., Baude P.F., Miller T.J., Haase M.A., Haugen G.M., Smekalin K. *Electron. Lett*., **32** (4) 345 (1996).
15. Kozlovsky V.I., Sannikov D.A., Sviridov D.E. *Bull. Lebedev Phys. Inst*., **35** (2), 35 (2008) [*Kratk. Soobshch. Fiz. FIAN*, **2**, 4 (2008)].
16. Butaev M.R., Kozlovsky V.I., Sannikov D.A., Skasyrsky Y.K. *J. Phys.: Conf. Ser*., **1439**, 012017 (2020).
17. Kozlovsky V.I., Kuznetsov P.I., Sviridov D.E., Yakusheva G.G. *Quantum Electron*., **42** (7), 583 (2012) [*Kvantovaya Elektron*., **42** (7), 583 (2012)].
18. Kozlovsky V.I. *Poluprovodnikovyi laser. Lazernye ELT, nanostructury dlya vidimogo i UF diapazonov* (Semiconductor Laser. Laser CRT, nanostructures for visible and UV regions); https://www.lap-publishing.com/catalog/details/store/it/book/978-3-659-33286-9/полупроводниковый-лазер.
19. Priller H., Schmidt M., Dremel M., Grün M., Toropov A., Ivchenko E.L., Kalt H., Klingshirn C. *Phys. Stat. Sol. (c)*, **1** (4) 747 (2004).